*33rd EPS Conference on Plasma Phys. Rome, 19 - 23 June 2006 ECA Vol.**30I**, P-4.164 (2006)*

Assessment of the trapped particle confinement in optimized stellarators*

V.V. Nemov[1], W. Kernbichler[2], S.V. Kasilov[1], G.O. Leitold[2], L.P. Ku[3]

[1] *Institute of Plasma Physics, National Science Center "Kharkov Institute of Physics and Technology", Akademicheskaya Str. 1, 61108 Kharkov, Ukraine*

[2] *Institut für Theoretische Physik, Technische Universität Graz, Petersgasse 16, A–8010 Graz, Austria*

[3] *Princeton Plasma Physics Laboratory, Princeton, New Jersey*

Introduction

A number of optimized stellarator configurations are analyzed with respect to trapped particle confinement using new target functions [1] which are related to collisionless α-particle confinement. These functions are based on specific averages of the bounce averaged ∇B drift velocity of trapped particles across magnetic surfaces. Computations of such simplified criteria require smaller computing times than direct computations of particle losses. An essential part of calculations relates to some new versions of the NCSX configuration. For comparison, computations for different types of stellarator configurations are performed. In addition, the poloidal drift of trapped particles is calculated with the aim to identify particles with vanishing poloidal drift velocity. This is of interest since such particles can be quickly lost from the plasma.

Basic formulas

The main optimization target introduced in [1] is the mean-square average over the pitch angle and over the magnetic surface of the bounce averaged ∇B drift velocity of trapped particles across magnetic surfaces,

$$\hat{\nu}_{\rm an} = \frac{1}{2\sqrt{2}}\,\Gamma_\nu\,\frac{\rho_L}{R_0}\nu\,, \tag{1}$$

with $\rho_L = v/\omega_{c0}$ being the characteristic Larmor radius and R_0 being the major radius of the torus. The dimensionless factor Γ_ν manifests the role of a specific magnetic configuration,

$$\Gamma_\nu = \sqrt{\frac{\Gamma_w}{\Gamma_s}}, \qquad \Gamma_s = \frac{\pi}{2\sqrt{2}}\frac{1}{\langle|\nabla\psi|\rangle}\left\langle|\nabla\psi|\sqrt{1-\frac{B}{B^{abs}_{max}}}\right\rangle, \tag{2}$$

$$\Gamma_w = \frac{\pi R_0^2}{\sqrt{2}}\lim_{L_s\to\infty}\left(\int_0^{L_s}\frac{ds}{B}\right)^{-1}\frac{1}{\langle|\nabla\psi|\rangle^2}\int_{B^{abs}_{min}/B_0}^{B^{abs}_{max}/B_0} db'\sum_{j=1}^{j_{max}}\left(\frac{dg_j}{db'}\right)^2\left(\frac{d\hat{I}_j}{db'}\right)^{-1}. \tag{3}$$

Here, ψ is the magnetic surface label, B_0 is the reference magnetic field and B^{abs}_{min} and B^{abs}_{max} are the absolute minimum and maximum of B within the sufficiently large interval of s, $[0, L_s]$,

*This work has been carried out within the Association EURATOM-ÖAW and with funding from the Austrian Science Fund (FWF) under contract P16797-N08.

respectively (s is the length along the magnetic field line). The index j is numbering the field line intervals $[s_j^{min}, s_j^{max}]$ where $b' - B/B_0 \geq 0$, $b' = v^2/(J_\perp B_0)$. $\langle A \rangle$ denotes the flux surface average for A. The quantities g_j and $\hat{I}_j$ are determined as

$$g_j = \frac{1}{3} \int_{s_j^{min}}^{s_j^{max}} \frac{\mathrm{d}s}{B} \sqrt{1 - \frac{B}{B_0 b'}} \left(4\frac{B_0}{B} - \frac{1}{b'} \right) |\nabla\psi| k_G, \quad \hat{I}_j = \int_{s_j^{min}}^{s_j^{max}} \frac{\mathrm{d}s}{B} \sqrt{1 - \frac{B}{B_0 b'}}, \tag{4}$$

with k_G being the geodesic curvature of the magnetic field line. The representation in (3) has the advantage that it can be computed efficiently in a field line tracing code. For a specific configuration, Γ_v is only a function of the minor radius. Minimization of Γ_v corresponds to the optimization of the trapped particle collisionless confinement.

Computations of Γ_v

Using Boozer spectra for B and for cylindrical coordinates of magnetic surfaces, computations of Γ_v are carried out for two sets of magnetic configurations of NCSX (e04, e04003, e04T8G, e04T8H and N3A0, N3AKB, N3ARAB, respectively). These configurations are results of further optimizations of configurations presented in Ref. [2]. For comparison, computations are also done for the standard and the high mirror configurations of W7-X (w7x-sc1 and w7x-hm1, respectively), two LHD inward shifted configurations [3] (for R_{ax}=3.6 and 3.53 m, R_{ax} is a major radius of the magnetic axis), and an optimized quasi-isodynamical stellarator configuration (QI-opt) with poloidally closed contours of B on magnetic surfaces [4].

Computational results for NCSX are presented in Figs. 1 and 2, whereas results for the other configurations together with the best NCSX configuration are presented in Fig. 3. From Figs. 1 and 2 follows that for NCSX the best results are realized for configurations e04003 from the 1^{st} set and N3ARAB from the 2^{nd} set. In a wide interval of r/a N3ARAB is the best configuration. For a classical stellarator Γ_v is close to unity [1]. One can clearly see, that Γ_v for N3ARAB in the whole volume is improved by a factor of more than 5 compared to a classical stellarator. In the range $0.35 \leq r/a \leq 0.8$ the improvement is even more than a factor of 10.

For LHD with R_{ax}=3.6 m (σ optimized [5] for $r/a \approx 0.5$) Γ_v is only $2 \div 2.5$ times smaller than for a classical stellarator. For LHD with R_{ax}=3.53 m (neoclassical-transport-optimized configuration of LHD [5]) for $r/a \geq 0.5$ Γ_v is ≈ 2.5 times smaller than unity (except for the near-boundary layer). The W7-X configurations are slightly better in this respect. The minimum Γ_v values are found to be about 3 and 4 times smaller than unity (high-mirror and the standard configurations, respectively) for $r/a \approx 0.7$. Beside the improved NCSX version, the QI-opt configuration is the best one in the range $r/a < 0.95$.

Computations of the poloidal drift of trapped particles

The poloidal motion of trapped particles $d\theta/dt$ is computed using Eq. (55) of Ref.[1] with the radial electric field being zero. The results are analyzed in a normalized form $d\theta/dt_{\mathrm{norm}}$. For normalization, $d\theta/dt$ for a deeply trapped particle near the magnetic axis of an l=2 stellarator

is used. Characteristic results are presented which are chosen from computations for the first 90 minima of B along a magnetic field line. The results cover roughly one toroidal period.

Figures 4 to 6 show results for $d\theta/dt_{\mathrm{norm}}$ as functions of the pitch $\gamma=v_{\|0}/v_{\perp 0}$ for ncsx-N3ARAB, w7x-hm1 and QI-opt, respectively. Here, $v_{\|0}$ is $v_{\|}$ at a local minimum of B and $v_{\perp 0}=\sqrt{J_{\perp}B_0}$. The curves for $d\theta/dt_{\mathrm{norm}}$ are marked according to the numbering of the minima of B/B_0 along the magnetic field lines which are also presented in the figures. Here, n is the number of integration steps with 1280 steps per magnetic field period. In addition, plots for γ_c as functions of γ are shown. The γ_c quantity represents the angle (in $\pi/2$ units) between a magnetic surface cross-section and a contour of $J_{\|}$=const in the point where these two curves cross each other. The γ_c value is calculated as $\gamma_c=(2/\pi)\arctan(v_{\mathrm{an}}/rd\theta/dt)$ where v_{an} is the bounce averaged radial drift velocity of a trapped particle calculated with formula (16) of Ref. [1]. When $d\theta/dt$ approaches zero, $\gamma_c\approx\pm 1$ which corresponds to a condition where the $J_{\|}$=const contour is perpendicular to the magnetic surface. With high probability this corresponds to $J_{\|}$=const contours which are not closed and this, in turn, leads to quick losses of the corresponding trapped particles.

It follows from Fig. 4 that for ncsx-N3ARAB ($r/a\approx 0.8$), $d\theta/dt_{\mathrm{norm}}$ is close to zero for deeply trapped particles (small γ) in those local minima of B which are located in the lower regions of the B/B_0 distribution. For smaller values of r/a (the results are not shown in the figures here) the general property is that trapped particles corresponding to higher regions of the B/B_0 distribution have $d\theta/dt>0$. At the same time, particles trapped near the local minima of B in the lower regions of B/B_0 have $d\theta/dt<0$. So, with increasing γ for all trapped particles of such a kind $d\theta/dt$ turns into zero for a certain value of γ. Figure 5 shows characteristic results for the high-mirror configuration of W7-X ($r/a\approx 0.56$). For a rather big fraction of minima of B, $|\gamma_c|$ is close to unity but the γ intervals corresponding to such values of $|\gamma_c|$ are small. Figure 6 shows results for poloidal motion in QI-opt for $r/a\approx 0.84$. For this surface $d\theta/dt\neq 0$ for all minima of B and for a majority of these minima γ_c is smaller than 0.2. Such and even better results are realized for surfaces corresponding to smaller values of r/a. For surfaces with $r/a>0.84$ trapped particles with $d\theta/dt=0$ appear. For example, at $r/a=0.91$ six minima from 90 have values of $d\theta/dt=0$.

From computations for LHD, R_{ax}=3.53 m, (the results are not shown here) it follows that for $r/a\approx 0.49$ trapped particles with $d\theta/dt=0$ exist only for the deepest ripple wells for γ close to the trapping boundary in such a ripple. With increasing r/a to $r/a\approx 0.7$ the trapped particles corresponding to $d\theta/dt=0$ disappear.

Conclusion

The employed technique has the advantage that the computations can be efficiently performed using a field line tracing code. From the computations it follows that for the N3ARAB configuration of NCSX the averaged radial ∇B drift velocity of trapped particles is smaller than for an equivalent classical stellarator by more than a factor of five in total. This is the best

result in the comparison with other optimized stellarator configurations. A numerical analysis of velocities of the radial drift as well as the poloidal drift allows for a quick assessment of $J_{||}$ contours in the vicinity of a given magnetic surface. Contours of $J_{||}$=const perpendicular to magnetic surfaces are found for the majority of the configurations. An exception is only the inner part of the QI-opt configuration. However, the intervals of pitches for the corresponding trapped particles are small and the fractions of such particles are expected to be small.

References

[1] V. V. Nemov et al., Phys. Plasmas **12**, 112507 (2005).

[2] L. P. Ku and the ARIES-CS Team, *20th IEEE/NPSS Symposium on Fusion Engineering, San Diego, CA, 14-17 October 2003* (IEEE, New York, 2003), p.312.

[3] V. V. Nemov et al., *32nd EPS Conference on Plasma Physics* , Tarragona, 27 June - 1 July 2005, ECA Vol. **29C**, P-1.110 (2005).

[4] A. A. Subbotin et al., *29th EPS Conference on Plasma Phys. and Contr. Fusion*, Montreux, Switzerland, 17-21 June 2002, ECA Vol. **26B**, P5.086 (2002).

[5] S. Murakami et al., *Nucl. Fusion* **42**, L19 (2002).

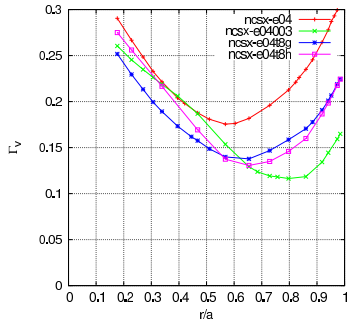

Fig. 1

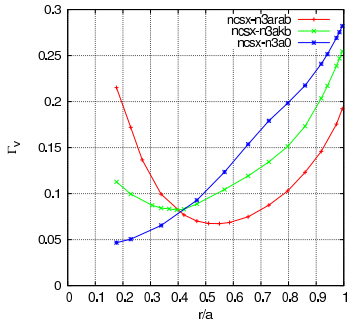

Fig. 2

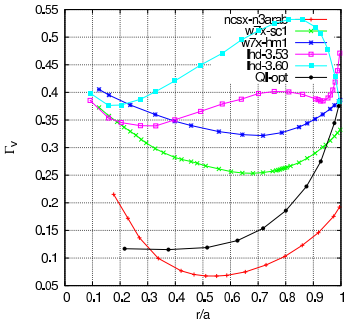

Fig. 3

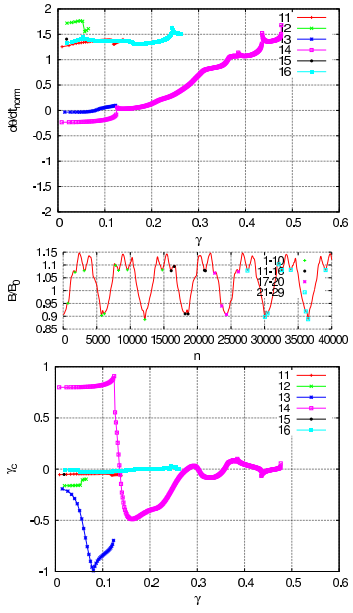

Fig. 4:
n3arab, r/a=0.797

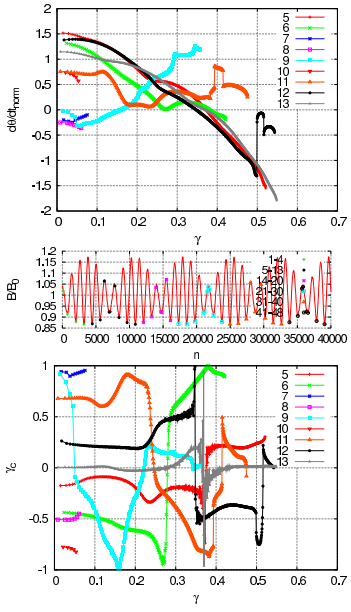

Fig. 5:
w7x-hm1, r/a=0.558

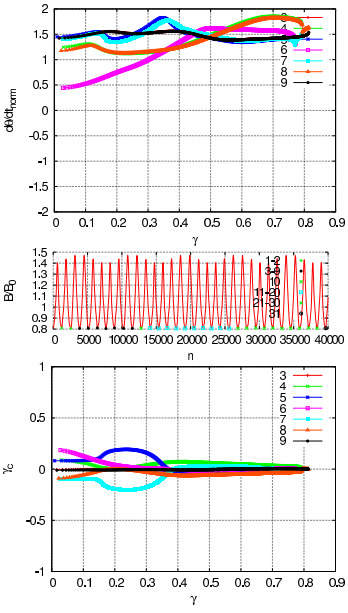

Fig. 6:
QI-opt, r/a=0.838